Conference Paper, Published Version

Altinakar, Mustafa; Evangelista, S.; Leopardi, Angelo

GMUSTA method for numerical simulation of dam break flow on mobile bed

River Flow 2010 - Dittrich, Koll, Aberle & Geisenhainer (eds) - © 2010 Bundesanstalt für Wasserbau ISBN 978-3-939230-00-7

GMUSTA method for numerical simulation of dam break flow on mobile bed

M. S. Altinakar
National Center for Computational Hydroscience and Engineering, University of Mississippi, Oxford MS, USA

S. Evangelista
Università degli Studi di Cassino, Cassino, Italy (visiting scholar at NCCHE, UM, Oxford, MS)

A. Leopardi
Università degli Studi di Cassino, Cassino, Italy

ABSTRACT: A two-phase morphodynamic model has been developed to simulate dam-break wave on a mobile bed. The numerical implementation of such a model using classical upwind methods remains a challenging task due to the complexity of developing a suitable Riemann solver for multi-phase flow problems. The present study employs the GMUSTA method to compute the numerical intercell fluxes, which is simpler and avoids the solution of the Riemann Problem in the conventional sense. GMUSTA is a multi-stage centered-scheme for constructing numerical intercell fluxes using a local grid around the interface. It is capable of reproducing the high accuracy of upwind schemes while keeping the simplicity of centered schemes. Several laboratory experiments of dam-break wave over a mobile bed from the literature were simulated using a one-stage GMUSTA implementation. The numerical results obtained with the GMUSTA method were compared against those obtained using a second-order accurate classic finite-volume implementation of the same mathematical model and the measured experimental data. It is shown that the numerical results obtained through a 1-stage GMUSTA implementation give a good agreement with the experimental results. A significant improvement is achieved with respect to the classic upwind method in terms of simplicity and computational efficiency.

Keywords: Dam break, mobile bed, numerical methods, GMUSTA

1 INTRODUCTION

The propagation of a dam-break wave over a mobile bed has been the subject of several research studies in the last few years. Due to its very rich and complex behavior, the propagation of dam-break waves over a mobile bed has recently gained the status of a standard benchmark for developing innovative solid transport models (e.g. Zech et al., 2004). From a physical point of view, the special features of the process suggest abandoning the hypothesis of immediate adaptation of solid transport to changes in hydrodynamics in favor of adopting non-equilibrium formulations, which are likely to provide a more accurate description (Fraccarollo & Capart, 2002, Greco et al., 2008). From the numerical standpoint, the accurate tracking of the water and bed wave-fronts requires adequate numerical schemes (e.g. Fraccarollo et al., 2003).

However, the development of new morphodynamic models (two-layers or two-phases) remains a difficult task due to the complexity of the eigenstructure. The main aim of the present work is to present a way to circumvent this difficulty by using a recent innovative numerical scheme.

A two-phase morphodynamic model (Greco et al., 2008) has been considered here to simulate dam break on a mobile bed. The implementation using classic upwind methods remains a challenging task due to the complexity of the use of the Riemann solvers in multi-phase flow problems. Hence, the present study employs the GMUSTA method by Toro & Titarev (2006) to compute the numerical intercell fluxes. This method is considerably simpler and avoids the necessity of solving a generalized Riemann Problem.

GMUSTA is a first-order multi-stage centered-scheme meant to be capable of reproducing the high accuracy of upwind schemes while keeping the simplicity and generality of centered schemes. It calculates the intercell fluxes as a particular average of symmetric fluxes, namely a weighted average of the Lax-Friedrichs and Lax-Wendroff fluxes (*GFORCE flux*), passing through predictor and corrector steps (*MUSTA approach*).

Simulations of laboratory experiments from the literature have been carried out using a one-stage GMUSTA method. The numerical results obtained with GMUSTA have been compared against measured experimental data and numerical results given by a second-order accurate finite volume implementation of the same mathematical model, which requires a numerical viscosity in order to damp spurious oscillations.
It will be shown in the following that the numerical results obtained through a one-stage MUSTA implementation show a good agreement with the experimental results. A significant improvement is also achieved with respect to the classical upwind method in terms of simplicity and computational efficiency.

2 THE MORPHODYNAMIC MODEL

2.1 *The Model*

The morphodynamic model proposed by Greco et al. (2008) is used here. It is a two-phase model, whose equations express mass and momentum conservation with reference to water and sediments separately. Here these equations are written in a 1D framework for sake of simplicity.

Conservation of total mass and of sediment mass leads to:

$$\frac{\partial h}{\partial t}+\frac{\partial (Q+Q_S)}{\partial x}+\frac{\partial Z}{\partial t}=0 \tag{1}$$

$$\frac{\partial \delta}{\partial t}+\frac{\partial Q_S}{\partial x}+(1-p)\frac{\partial Z}{\partial t}=0 \tag{2}$$

in which t is time, x is the abscissa, Q and Q_s are the water and the solid discharge for unit width, respectively, h is the total flow depth, Z is the bottom elevation above a datum, δ is the ratio of sediment volume to base area and p is the bed porosity.

Water and sediment momentum equations are written separately:

$$\frac{\partial Q}{\partial t}+\frac{\partial}{\partial x}\left(\frac{Q^2}{(h-\delta)}+g\frac{h^2}{2}\right)+gh\left(\frac{\partial Z}{\partial x}+S_f\right)=0 \tag{3}$$

$$\frac{\partial Q_S}{\partial t}+\frac{\partial}{\partial x}\left(\frac{{Q_S}^2}{\delta}+\frac{g\Delta}{C(\Delta+1)}\frac{\delta^2}{2}\right)+ +g\delta\frac{\Delta}{\Delta+1}\frac{\partial Z}{\partial x}+S_s=0 \tag{4}$$

where S_f and S_s denote the water and sediment momentum source/sink terms, respectively, g is gravity, ρ and ρ_s are the water and sediment density, respectively, $\Delta = (\rho_s-\rho)/\rho$ and C is the solids concentration (assumed as a constant).

The water source term S_f is computed as the sum of the bottom friction (evaluated using a uniform flow formula like Chezy's) and the drag exchanged between the two phases:

$$S_f=\left(\frac{{U_w}^2}{{C_h}^2}+\frac{Drag}{\rho}\right)\frac{1}{gh},$$

where U_w is the average water velocity, C_h is the non-dimensional Chezy coefficient, *Drag* is the drag force exchanged between the two phases.
The corresponding solid source term S_s accounts for drag exchange and the collisional shear stress computed, after Bagnold, as a coefficient α multiplied by the square of the particle velocity U_s:

$$S_s=\alpha {U_s}^2-\frac{Drag}{\rho_s}.$$

The fifth and last equation relates the bottom evolution to the mass exchange with the flow, e_b and reads:

$$\frac{\partial Z}{\partial t}=-e_b \tag{5}$$

A closure relation for the entrainment/deposition term e_b is then required. Greco et al. (2008) assumed that entrainment occurs due to the unbalance among the sum of stresses exerted on the bed by water phase (Chezy) and solid phase (Bagnold) and the attrition among solid particles belonging to the bed:

$$e_b=\frac{\tau_w+\tau_s-\tau_b}{c_{sc}(\rho_s-\rho)\cdot\max(w_s,U_s)},$$

where $\tau_w=\rho {U_w}^2/{C_h}^2$ and $\tau_s=\rho_s\alpha {U_s}^2$ are, respectively the stresses exerted by the water and by the solid phase and $\tau_b=(\rho_s-\rho)g\delta\ tg\varphi$ is the attrition among solid particles belonging to the bed, with C_{sc} an empirical coefficient determined by calibration, φ the sediment friction angle and w_s the particle free fall velocity.

Model parameters are then the drag coefficient (C_d) that accounts for momentum transfer between water and solid phases, the Bagnold α coefficient, the non-dimensional Chezy coefficient (C_h) and the internal friction angle (φ). More details are given in the original paper by the Authors (Greco et al., 2008).

2.2 *Eigenstructure of the Model*

Equations (1) – (4) are a system of conservation laws since equation (5) can be substituted in (1) and (2). They can be written in the *conservative matricial form* as

$$\mathrm{Q}_t + \mathrm{F}_x(\mathrm{Q}) = \mathrm{S}(\mathrm{Q}), \tag{6}$$

where:

$$\mathrm{Q} = \begin{pmatrix} h \\ \delta \\ Q \\ Q_S \end{pmatrix}, \qquad \mathrm{F}(\mathrm{Q}) = \begin{pmatrix} Q + Q_S \\ Q_S \\ \dfrac{Q^2}{h-\delta} + g\dfrac{h^2}{2} \\ \dfrac{{Q_S}^2}{\delta} + g\ \dfrac{\delta}{C}\dfrac{\Delta}{\Delta+1}\dfrac{\delta^2}{2} \end{pmatrix},$$

$$\mathrm{S}(\mathrm{Q}) = \begin{pmatrix} e_b \\ (1-p)\, e_b \\ -gh\left(\dfrac{\partial Z}{\partial x} + S_f\right) \\ -g\delta\dfrac{\Delta}{\Delta+1}\dfrac{\partial Z}{\partial x} - S_s \end{pmatrix}$$

are, respectively, the vector of *conserved variables*, the vector of *fluxes* and the vector of *source terms*. Q_t and $\mathrm{F}_x(\mathrm{Q})$ are, respectively, the time derivative of the vector of conserved variables and the space derivative of the flux vector. As demonstrated in the paper by Greco et al. (2008), the model (1) – (4) is strictly hyperbolic and its eigenvalues are:

$$\lambda_{1,2} = U_w \cdot \left(1 \pm \frac{1}{Fr}\right); \qquad \lambda_{3,4} = U_s \cdot \left(1 \pm \frac{1}{Fr_s}\right)$$

where U_w and U_s are water and solids phases velocities and F_r and F_{rs} are peculiar Froude numbers:

$$F_r = \frac{U_w}{\sqrt{gh}}; \; F_{rs} = \frac{U_s}{\sqrt{g\dfrac{\delta}{C}\dfrac{\Delta}{\Delta+1}}}.$$

Because of the hyperbolicity of this system of equations, numerical methods for conservation laws can be applied for the numerical integration of the model (Toro, 2009).

3 GMUSTA METHOD

3.1 *Selection of the method*

Application of conservative Godunov schemes for solving systems of conservation laws requires the use of a suitable Riemann solver. However this task can be quite involved in multi-phase problems due to the complexity of the eigenstructure of the model, such as the one presented in section 2.2. In fact for 2-equation problems, such as clear-water dam-break wave propagation over a fixed bed, it is easy to identify the so-called "*star region*" and, therefore, the solution of the Riemann Problem. However, when the number of equations is higher, this may become quite complicated. Moreover the coupling between the two phases (solid and liquid) renders the task of writing Riemann invariants very difficult.

Thus, numerical techniques which avoid the solution of the Riemann Problem in the conventional sense appear more appropriate in terms of the simplicity of their implementation and their computational efficiency. Centered schemes allow the resolution of the Riemann Problem to be avoided, but they are in general not as accurate as upwind methods, which are widely considered, within the class of existing *monotone first-order fluxes*, the best in terms of accuracy (Toro, 2009). However, the superior accuracy of upwind methods comes at the cost of the necessity of solving exactly or approximately the Riemann Problem.

The GMUSTA method (Toro & Titarev, 2006) is a first-order centered scheme, which achieves the accuracy of upwind methods by incorporating the GFORCE flux into the MUSTA approach using predictor and corrector steps.

Since the eigenstructure of the system (1) - (4) of non-linear hyperbolic equations is not completely available, the application of the GMUSTA method is of great utility in this case. The scheme may be interpreted as an "unconventional approximate Riemann solver" that has simplicity and generality as its main features.

3.2 *Description of the method*

The finite volume scheme to solve the generic $m \times m$ one-dimensional homogeneous system of hyperbolic conservation laws, given as

$$\mathrm{Q}_t + \mathrm{F}_x(\mathrm{Q}) = 0, \tag{7}$$

where Q is the vector of the m conserved variables and F(Q) the corresponding vector of fluxes, reads:

$$\mathrm{Q}_i^{n+1} = \mathrm{Q}_i^n - \frac{\Delta t}{\Delta x}\left[\mathrm{F}_{i+1/2} - \mathrm{F}_{i-1/2}\right], \tag{8}$$

in which i is the cell index, n is the time index, Δt is the time step and Δx the space step.

Given two adjacent data states Q_i^n and Q_{i+1}^n, the corresponding intercell numerical flux $\mathrm{F}_{i+1/2}$ at the interface $i+1/2$ is evaluated as a *GFORCE flux* (Toro, 2006), a weighted average of the Lax-Friedrichs and Lax-Wendroff fluxes. It is then incorporated in the framework of the *MUSTA ap-*

proach, resulting in a version of the method called *GMUSTA*.

The GFORCE flux is given by:

$$\mathrm{F}_{i+1/2}{}^{GFORCE} = \omega_g \cdot \mathrm{F}_{i+1/2}{}^{LW} + \left(1-\omega_g\right)\cdot \mathrm{F}_{i+1/2}{}^{LF}, \qquad (9)$$

where:

$$\mathrm{F}_{i+1/2}{}^{LW} = \mathrm{F}\left(\mathrm{Q}_{i+1/2}{}^{LW}\right)$$

is the Lax-Wendroff flux, with:

$$\mathrm{Q}_{i+1/2}{}^{LW} = \frac{1}{2}\left[\mathrm{Q}_i{}^n + \mathrm{Q}_{i+1}{}^n\right] - \frac{1}{2}\frac{\Delta t}{\Delta x}\left[\mathrm{F}\left(\mathrm{Q}_{i+1}{}^n\right) - \mathrm{F}\left(\mathrm{Q}_i{}^n\right)\right],$$

and

$$\mathrm{F}_{i+1/2}{}^{LF} = \frac{1}{2}\left[\mathrm{F}\left(\mathrm{Q}_i{}^n\right) + \mathrm{F}\left(\mathrm{Q}_{i+1}{}^n\right)\right] - \frac{1}{2}\frac{\Delta x}{\Delta t}\left[\mathrm{Q}_{i+1}{}^n - \mathrm{Q}_i{}^n\right]$$

is the Lax-Friedrichs flux, with $\omega_g = 1/\left(1+CFL\right)$, where *CFL* is a prescribed Courant number such that $0 \le CFL \le 1$.

In the MUSTA multi-stage approach, the numerical flux $\mathrm{F}_{i+1/2}$ for the conservative scheme is found by first approximating numerically the solution of the corresponding Riemann Problem to produce two modified states on either side of the cell interface (*predictor step*). In the *corrector step* the intercell numerical flux is corrected by evaluating a numerical flux function at the two modified states of the predictor step.

The solution of the Riemann Problem is approximated numerically through a separate, independent mesh called the MUSTA mesh, on a $d-\tau$ plane of independent variables, where *d* denotes the spatial variable, associated with *x*, and τ denotes the temporal variable, associated with *t*.

In Figure 1 the separate frame in the $d-\tau$ plane corresponding to the interface $x_{i+1/2}$ is represented. The $d-$axis is discretized into an integer number of *M* cells of regular size Δd. The states $\mathrm{Q}_i{}^n$ and $\mathrm{Q}_{i+1}{}^n$ are associated with the mesh points 0 and 1: the cells i and $i+1$ in $x-t$ plane correspond, respectively, to cells 0 and 1 on the MUSTA mesh, so that the intercell position $i+1/2$ corresponds to the interface $1/2$.

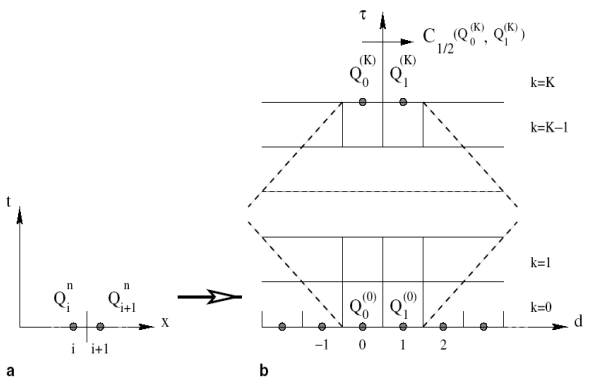

Figure 1. Correspondence between the computational and MUSTA meshes in the MUSTA approach. [Toro & Titarev, 2006]

The initial condition for the numerical problem on the MUSTA mesh is:

$$\mathrm{Q}_l{}^{(0)} = \begin{cases} \mathrm{Q}_i{}^n & \text{if } l \le 0 \\ \mathrm{Q}_{i+1}{}^n & \text{if } l \ge 1 \end{cases}, \qquad (10)$$

where *l* is the cell index.

The $\tau-$time evolution of the problem (or *multi-staging*) is performed via the conservative scheme:

$$\mathrm{Q}_l{}^{k+1} = \mathrm{Q}_l{}^k - \frac{\Delta t}{\Delta d}\left[\mathrm{P}_{l+1/2}{}^k - \mathrm{P}_{l-1/2}{}^k\right], \qquad (11)$$

where $\Delta\tau$ is the time step in the MUSTA mesh and $\mathrm{P}(\mathrm{V}_L,\mathrm{V}_R)$, is a two-point monotone numerical flux for the MUSTA mesh, called the *predictor flux*. One usually takes $\Delta d = 1$. The MUSTA time step $\Delta\tau$ is computed as $\Delta\tau = C_{musta}\,\Delta d / S_{musta}{}^{(k)}$, where C_{musta} is the *CFL* coefficient and $S_{musta}{}^{(k)}$ is the maximum signal speed in the MUSTA mesh at stage *k*. In the examined problem, in particular,

$$S_{musta}{}^{(k)} = U_w\left(1+\frac{1}{F_r}\right)$$

After a total number of stages *K*, i.e. *K*+1 time steps along the τ axis, the predictor procedure yields two new states $\mathrm{Q}_0{}^{(K)}$ and $\mathrm{Q}_1{}^{(K)}$ on either side of the cell interface in the MUSTA mesh, which are evolved from the initial states $\mathrm{Q}_0{}^{(0)} = \mathrm{Q}_1{}^n$ and $\mathrm{Q}_1{}^{(0)} = \mathrm{Q}_{i+1}{}^n$.

For a sufficiently large number of stages and a convergent scheme (11) one would obtain an approximation to the solution of the Riemann Problem at two positions left and right close to the interface position, not at the interface itself. In order to obtain a numerical flux at the interface itself a corrector stage is performed, whereby the evolved data $(\mathrm{Q}_0{}^{(K)}, \mathrm{Q}_1{}^{(K)})$ is resolved via a two-point, monotone numerical flux $\mathrm{C}(\mathrm{V}_L,\mathrm{V}_R)$, called the *corrector flux*. In this manner the sought intercell numerical flux $\mathrm{F}_{i+1/2}$ for use in the conservative scheme (8) is found:

$$\mathrm{F}_{i+1/2}{}^{MUSTA-K} = \mathrm{C}_{1/2}\left(\mathrm{Q}_0{}^{(K)}, \mathrm{Q}_1{}^{(K)}\right).$$

In this paper the number of multi-stages *K* chosen for the calculation is equal to 1 (i.e. GMUSTA-1), as suggested by Toro & Titarev (2006) for practical applications. The gains to be obtained by using 2 or 3 stages (GMUSTA-2 and GMUSTA-3) do not seem to justify the extra expense in calculation.

The GMUSTA−1 scheme is illustrated in Figure 2. The initial data is prescribed in the domain of just two cells, namely $l = 0$ and $l = 1$. The boundary fluxes $\mathrm{P}_{-1/2}{}^{(0)}$ and $\mathrm{P}_{3/2}{}^{(0)}$ are computed on the initial data, namely $\mathrm{P}_{-1/2}{}^{(0)} = \mathrm{F}(\mathrm{Q}_0{}^{(0)})$ and $\mathrm{P}_{3/2}{}^{(0)}$

= $F(Q_1^{(0)})$. The only non-trivial flux is $P_{-1/2}^{(0)}$. Using (8), the vectors $Q_0^{(0)}$ and $Q_1^{(0)}$ will be evolved as:

$$Q_0^{(1)} = Q_0^{(0)} - \Delta\tau^{(0)}\left[P_{-1/2}^{(0)} - P_{1/2}^{(0)}\right] \quad \text{(left cell)}$$

$$Q_1^{(1)} = Q_1^{(0)} - \Delta\tau^{(0)}\left[P_{3/2}^{(0)} - P_{1/2}^{(0)}\right]. \quad \text{(right cell)}$$

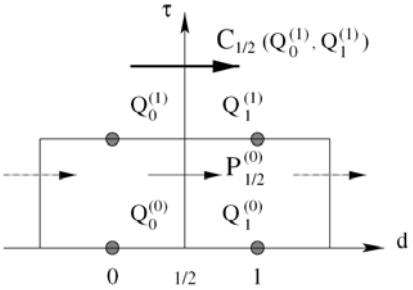

Figure 2. One-stage MUSTA-1 scheme (K=1). [Toro & Titarev, 2006]

The spacing has been set as $\Delta d = 1$ and $\Delta\tau^{(0)}$ is the size of the stable time step calculated on the initial data ($Q_0^{(0)}$, $Q_1^{(0)}$).

As $K = 1$, the multi-staging is complete and the sought numerical flux is simply obtained by applying a corrector flux $C(V_L, V_R)$ to the evolved data $Q_0^{(1)}$ and $Q_1^{(1)}$:

$$F_{i+1/2}^{MUSTA-1} = C_{1/2}\left(Q_0^{(1)}, Q_1^{(1)}\right).$$

Treatment of source terms is performed using a fractional step approach (Leveque, 2002).

4 NUMERICAL RESULTS

4.1 *Simulations and experimental data for comparison*

A numerical implementation of the morphodynamic model has been performed using a GMUSTA-1 scheme. It allows performing simulations of sample phenomena of dam break on movable and fixed bed for one-dimensional and two-dimensional cases.

A large number of simulations were performed with GMUSTA-1 taking into account different boundary conditions and bed morphologies.

In this paragraph a comparison of the numerical results of a one-dimensional dam break against some experimental data are shown.

The experimental data are the ones collected during the experiences of Spinewine and Zech (2007). The bed is made of sand (d_{50} 1.82 mm) in the first case (Figure 3 and Figure 4) and spherical PVC particles (d_{50} 3.9 mm) in the second one (Figure 5).

A dam break is simulated starting from an initial water level of 0.35 m on a 8-m long horizontal channel, with a gate positioned in the middle.

4.2 *Sand tests*

The values of the parameters assumed for the calculation in the sand case are: time step $\Delta t = 0.005$ s, computational mesh space $\Delta x = 0.02$ m, MUSTA-mesh space $\Delta d = 1.00$ m, Courant number $CFL = 0.90$, water density $\rho = 1000$ kg/m^3, sediment density $\rho_s = 2680$ kg/m^3, water kinematic viscosity $\nu = 1.0\text{e-}06$ m^2/s, sediment internal friction angle $\varphi = 30°$, average sediment particles diameter $d_{50} = 0.00182$ m, average sediment volume concentration in the transport layer $C = 0.5$, bed porosity $p = 0.5$, Bagnold coefficient $\alpha = 0.07$, gravity $g = 9.81$ m/s^2, empirical factor scale for erosion $C_{sc} = 0.80$, Drag coefficient $C_d = 0.015$, non-dimensional Chezy coefficient $C_h = 30$.

Figure 3 shows the bottom profile, the interface between the transport layer and the clear water and the free surface, respectively, at 0.50, 1.00 and 1.50 s after the removal of the gate.

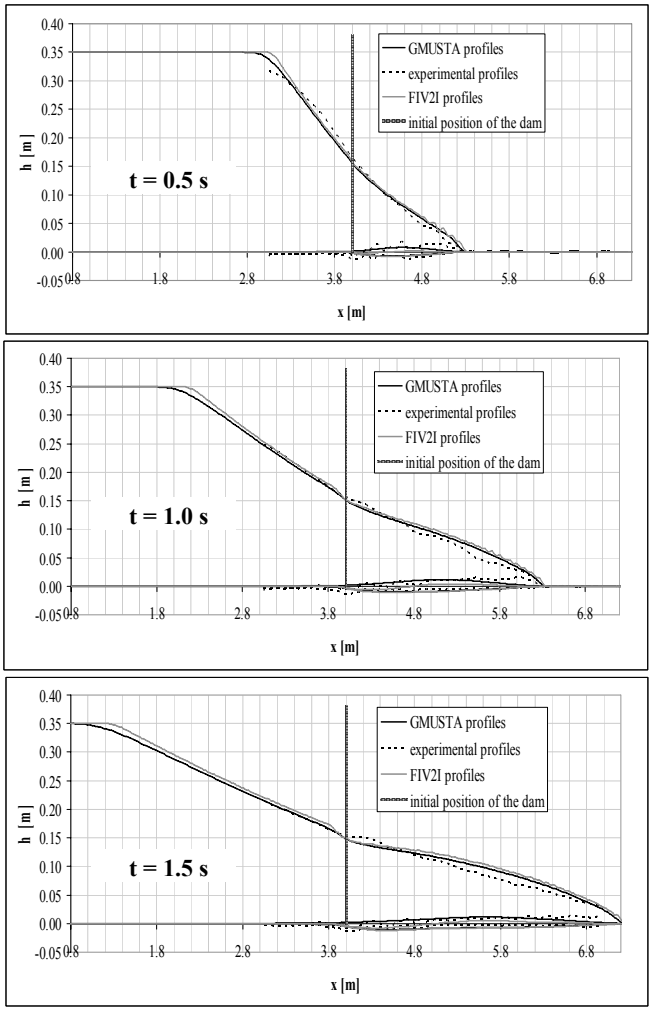

Figure 3. Comparison of GMUSTA numerical results against experimental data from Spinewine and Zech (sand d_{50} 1.82 mm) and FIV2I numerical results, respectively at 0.5, 1.0 and 1.5 s after the removal of the gate.

The numerical results obtained with GMUSTA-1 are also compared, for the case of sand bottom, against the ones obtained by the numerical technique used by Greco et al. (2008), which is based on a Finite Volume Second Order Interpolation Technique (FV2I) proposed by Leopardi (2001).

There is good agreement between the position of the wave front predicted by GMUSTA-1 and the experimental data, which is quite important in dam break problems. Many numerical models fail to predict the thickness of the transport layer correctly. It is interesting to note that the thickness predicted by GMUSTA-1 agrees quite well with the measured data.

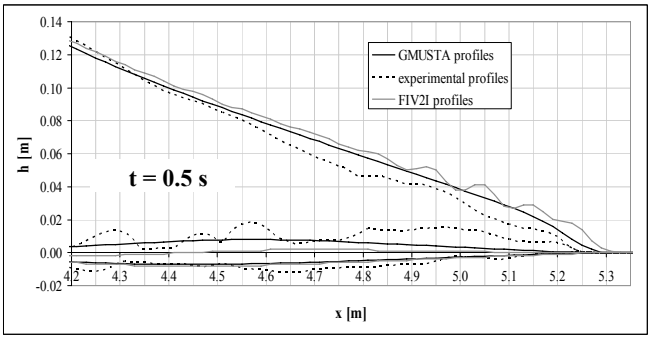

Figure 4. Detail of the wave front position: comparison of GMUSTA numerical results against experimental data from Spinewine and Zech (sand d_{50} 1.82 mm) and FIV2I numerical results at 0.5 s after the removal of the gate.

It is also evident that the numerical results obtained with GMUSTA-1 have a better accuracy than those obtained using FV2I. This is more evident in Figure 4, which shows in detail the wave front position at 0.5 s after the removal of the gate.

It is important to note that 1-stage GMUSTA method is computationally efficient and requires shorter computational time compared to FV2I.

4.3 *PVC tests*

The values of the parameters assumed for the calculation in the PVC case are: time step $\Delta t = 0.005$ s, computational mesh space $\Delta x = 0.02$ m, MUSTA-mesh cell size $\Delta d = 1.00$ m, Courant number $CFL = 0.90$, water density $\rho = 1000$ kg/m^3, sediment density $\rho_s = 1380$ kg/m^3, water kinematic viscosity $\nu = 1.0\text{e-}06$ m^2/s, sediment friction angle $\varphi = 38°$, average sediment particles diameter $d_{50} = 0.0039$ m, average sediment volume concentration in the transport layer $C = 0.5$, bed porosity $p = = 0.5$, Bagnold coefficient $\alpha = 0.075$, gravity g = 9.81 m/s^2, empirical factor scale for erosion $C_{sc} = 0.80$, Drag coefficient $C_d = 0.017$, Chezy coefficient $C_h = 30$.

In this case the prevision of the thickness of the transport layer is particularly satisfying, considering the fact that the PVC sediment particles have a diameter almost twice the size of the sand sediment particles.

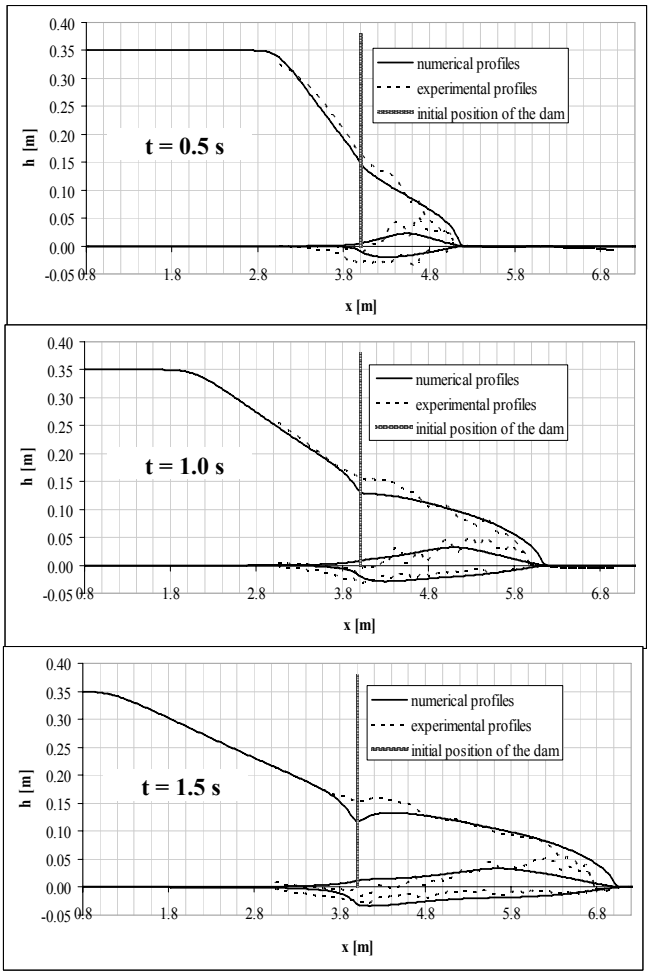

Figure 5. Comparison of numerical results against experimental data from Spinewine and Zech (PVC d_{50} 3.9 mm), respectively at 0.5, 1.0 and 1.5 s after the removal of the gate.

5 CONCLUSIONS

A two-phase morphodynamic model has been numerically implemented using the 1-stage GMUSTA method (GMUSTA-1) for the simulation of dam break flows on a mobile bed. The results have been compared against literature experimental data.

It is shown that the numerical results obtained through this 1-stage GMUSTA implementation give a good agreement with the experimental results. The good agreement between the simulation results and the experimental data proves that GMUSTA method allows a high accuracy despite its simplicity. The comparison with the implementation through a classical technique also shows a good accuracy and computational efficiency of the method.

LIST OF SYMBOLS

t time
x abscissa
h total flow depth
Q water discharge for unit width
Q_s solid discharge for unit width
Z bottom elevation above a datum
δ ratio of sediment volume to base area
p bed porosity
S_f water momentum source/sink term
S_s sediment momentum source/sink term
g gravity
ρ water density
ρ_s sediment density
$\Delta = (\rho_s-\rho)/\rho$
C solids concentration in the transport layer
α Bagnold coefficient
Drag drag force between the two phases
C_d drag coefficient
C_h non-dimensional Chezy coefficient
φ friction angle
e_b entrainment/deposition term
τ_w stress exerted by the water phase
τ_s stress exerted by the solid phase
τ_b attrition among solid particles of the bed
Q vector of the conserved variables
F(Q) vector of the fluxes
S(Q) vector of the source terms.
Q_t space derivative of the vector Q
$F_x(Q)$ time derivative of the vector F(Q)
U_w water velocity
U_s solid velocity
Fr Froude number for the water phase
Fr_s Froude number for the sediment phase
$\lambda_{1,2}$, $\lambda_{3,4}$ eigenvalues of the system of conservation laws
CFL Courant number
d, τ MUSTA mesh space and time variables
M number of cells
K number of stages
C_{musta} *CFL* coefficient in the MUSTA mesh
$S_{musta}^{(k)}$ maximum signal speed in the MUSTA mesh at stage k,
i cell index
n time index
Δt time step
Δx space step
d_{50} average sediment particles diameter
C_{sc} empirical factor scale for erosion
w_s particle free fall velocity

REFERENCES

Fraccarollo, L. and Capart, H. 2002. Riemann wave description of erosional dam-break flows. Journal of Fluid Mechanics, vol. 461, pp. 183-228.

Fraccarollo, L., Capart, H., Zech, Y. 2003. A Godunov method for the computation of erosional shallow water transients. International Journal for Numerical Methods in Fluids, 41, pp. 951-976.

Greco, M., Iervolino, M., Vacca, A., Leopardi, A. 2008. A two-phase model for sediment transport and bed evolution in unsteady river flow. River flow 2008, Çeşme, Izmir (Turkey), Vol. 1, pp. 669-677.

Leopardi, A. 2001. Modelli Bidimensionali di Corpi Idrici Naturali. PhD Thesis. University of Napoli "Federico II". (in Italian)

Randall J. Leveque 2002. Finite Volume Methods for Hyperbolic Problems, Cambridge University Press.

Spinewine, B., Zech, Y. 2007. Small-scale laboratory dam-break waves on movable beds. Journal of Hydraulic Research, Vol. 45 Extra Issue, pp. 73–86.

Toro, E. F. 1999. Riemann Solvers and Numerical Methods for Fluid Dynamics: A Practical Introduction. Second Edition, Springer-Verlag.

Toro, E. F. 2001. Shock-Capturing Methods for Free-Surface Shallow Flows, Wiley and Sons Ltd.

Toro, E. F., Titarev, V.A. 2006. MUSTA fluxes for systems of conservation laws, Journal of Computational Physics 216, pp. 403-429; DOI:10.1016/j.jcp.2005.12.012

Toro, E. F., Titarev, V.A. 2006. Derivative Riemann solvers for systems of conservation laws and ADER methods, Journal of Computational Physics 212, pp. 150-165; DOI:10.1016/j.jcp.2005.06.018

Toro, E. F. 2006. MUSTA: A multi-stage numerical flux. Applied Numerical Mathematics 56, pp. 1464-1479; DOI:10.1016/j.apnum.2006.03.022

Toro, E. F. 2009. Riemann Solvers and Numerical Methods for Fluid Dynamics: A Practical Introduction. Third Edition, Springer.

Zech ,Y., Soares Frazão, S., Spinewine, B., le Grelle, N. 2004. Dam-break induced flood modelling and sediment movement. IMPACT WP4 final scientific report. http://www.samui.co.uk/impact-project/default.htm